

GATE simulation of ^{12}C hadrontherapy treatment combined with a PET imaging system for dose monitoring: A feasibility study

Sébastien Jan, Thibault Frisson, and David Sarrut

Abstract—The GATE package is used to perform Monte Carlo hadrontherapy simulations of a cancer treatment combined with the complete description of an associated positron emission tomography (PET) imaging device for dose monitoring. This study aimed to demonstrate that the GATE platform has the capability to perform realistic simulations in the field of hadrontherapy, combining both dose and imaging system. We defined the simulation configuration as a carbon ion pencil beam scanning of a thorax CT phantom together with a complete PET imaging system. Two main positron emitters resulting from nuclear ^{12}C reactions are considered in this study: ^{11}C and ^{15}O . We studied the produced data to analyse the interest in using a full PET system simulation instead of the usual Gaussian smoothing applied on the positron emitters map. We found differences in the distal position of the signal falloff of 20% between full PET system simulation and the Gaussian model. We also studied the influence of the ^{15}O isotope in PET images and found the contribution to falloff of this isotope to be negligible (4%), which suggests the inclusion of ^{15}O isotope in the simulation is not necessary. Inally, we analysed the impact of dose delivery on PET image quality and found a difference of 20% on the PET estimation falloff between doses of 10 Gy and 1 Gy. This study shows that GATE, implemented on a computing system with large number of CPUs (≈ 1000), has the potential to be used for quantitative evaluation of imaging protocols for radiation monitoring.

Index Terms—Monte Carlo, GATE, Hadrontherapy, PET monitoring.

I. INTRODUCTION

Monte Carlo simulations are essential for many medical applications, especially for imaging and radiotherapy. Numerical approaches for imaging applications are used to design new devices, to optimise and study the effect of different acquisition parameters on image quality. They are also extremely useful to validate and assess compensation methods and image reconstruction techniques. Monte Carlo simulations are in general much slower than analytical methods but are considered the most precise simulation type. Moreover, they not only provide the dose distribution but also explicitly simulate nuclear interactions and secondary events, thus allowing the study of imaging systems such as hadronPET [1], which detect Beta+ emitters with a PET system, or prompt-gamma imaging. In radiation therapy, Monte Carlo simulations are used to develop fast dose deposition algorithms or to characterise

beam properties [2]. They are also the most used methods to study imaging detectors. The GATE [3], [4] open-source simulation platform, based on the Geant4 toolkit [5], [6], has been developed and used since 2002 by the OpenGATE collaboration. The work presented here considers PET as a method for *in situ* monitoring of carbon hadrontherapy. This method monitors the image of the radioactivity distribution induced by the nuclear fragmentation processes occurring during radiation [1]. Such distribution has been shown to be correlated with the dose distribution [7], leading to interesting perspectives in dose monitoring, even if exact quantification is still under study (e.g., the biological washout effects due to blood perfusion and metabolism deteriorate this correlation [8]). To our knowledge, GATE is the only Monte Carlo platform that allows simulation in the same framework of the whole range of physical events occurring during a hadron-PET scan. For example, GATE has already been used in PET imaging [9], [10] and in hadrontherapy dose simulations [4], [11].

The study described in this paper aimed to provide a proof of concept of the use of GATE to produce realistic simulations to estimate PET efficiency for therapeutic control in the case of hadrontherapy treatments. These simulations can be used to optimise the design of dedicated PET detectors and to identify the best protocols to control and follow the deposited dose.

II. METHOD

We defined a complete simulation setup that includes a model of a realistic ^{12}C pencil beam scanning, a numerical patient based on a thoracic CT scan, and a PET camera model for the image acquisition system. We considered in this study the production of ^{11}C and ^{15}O positron emitters resulting from nuclear ^{12}C reactions. We propose to illustrate the usability of GATE as a tool to study three main topics:

- The simulation of a full PET system simulation instead of the usual Gaussian smoothing applied on the positron emitters map;
- The impact and contribution of the ^{15}O isotope in the quantification of a PET image; and
- The relationship between PET image quality and the target deposited dose.

A. Two-step approach

We considered the simulation in two parts. The first part simulated the ^{12}C beam from the exit of the nozzle to the patient. Variables (energy, dose, position) were stored for primary

S. Jan is with the CEA/DSV/I²BM/SHFJ, 4 place Général Leclerc 91406 Orsay France.

D. Sarrut and T. Frisson are with the University of Lyon, CREATIS; CNRS UMR5220; INSA-Lyon, France and University of Lyon, Léon Bérard Cancer Center, F-69373, Lyon, France.

and secondary particles and especially for the distribution of β^+ emitters created during nuclear processes. We used a phase space to store the spatial distributions of all β^+ emitters created inside the computerised tomography (CT) target. The phase-space is binned such as to obtain three-dimensional (3D) maps describing the number of emitters inside each pixel of the CT image. These 3D maps were used as input files for the second part of the simulation, the PET scan acquisition. This two-step approach was designed to give users opportunities to test different configurations for the imaging system with the same deposited dose distribution. With this strategy, it is also possible to model an in-beam prompt-gamma dose monitoring strategy [12], [7] if information regarding the gamma prompts produced by ^{12}C nuclear reactions during tissue interactions is stored in dedicated files. This approach does not induce a penalty regarding the total computing time of the simulation.

B. Simulation setup: target and beam delivery

1) *CT target:* The simulation setup had the following geometry: The numerical phantom used in this study was a patient image of a four-dimensional (4D) CT thoracic acquisition available in the public domain [13]; this included a lung tumour on which an approximated gross tumour volume was manually delineated. No planning target volume was defined here. The target was defined as a thoracic CT image of a patient following conventional radiation therapy for non-small-cell lung cancer. The image was acquired on a Brilliance Big Bore 16-slice CT scanner (Philips Medical Systems, Cleveland, OH) with 120 kV, 400 mAs, and 0.15 pitch (because it is one phase of a 4D image). The original resolution was $0.97 \times 0.97 \times 2 \text{ mm}^3$, see fig 1. We resampled the image to isotropic 2^3 mm^3 voxel size (1.7 million voxels). The image was described in GATE with the method proposed in [14], allowing fast particle navigation through the matrix of voxels. Hounsfield units were converted into Geant4 materials thanks to the stoichiometric calibration method proposed in [15]. A density tolerance of 0.1 g/cm^3 was used, leading to 30 different Geant4 materials, with atomic composition interpolated from seven initial materials (air, lung, adipose tissue, adrenal gland, soft tissues, connective tissue, bone marrow) according to the mass density.



Fig. 1. Coronal slice of the thorax CT used in this study. The tumour target is clearly visible at the centre of the parenchyma on the right lung (left in the image).

2) *Physics list:* As recommended by the Geant4 electromagnetic (EM) standard working group for medical physics applications [16], we used the EM standard package with the list of parameters named option 3 (Opt3). The production range cuts were set to 0.1 mm for photon, electron, and positron. The maximum step size was set to 0.01 mm. The electron multiple scattering model was *Urban93*, which belong to the class of condensed simulations and uses model functions to determine the angular and spatial distribution after each step [5]. The option *fUseDistanceToBoundary* was turned on for multiple scattering of electrons and positrons. This option enables the use of particle range, geometrical safety and linear distance to geometrical boundary as step limitation [5]. The number of bins in physics tables was increased from 84 (default) to 220. The parameter *finalRange* used in the computation of step limit by the ionisation process was reduced with respect to the default value 1 mm: 0.1 mm for e+,e-; 0.05 mm for muons, pions, and proton; and 0.02 mm for ions. For the second part of the simulation focus on the imaging part, as no deposited dose is monitored, we applied a high production cut (10 mm) in the detector region, allowing to not generate the secondary electron. It does not change the results, and it provides a significant computing speed-up. Regarding hadronic interactions, we followed the recommendation of [17], [18], with one exception: we used the precompound as an inelastic hadronic model even above 80 MeV following [19], [20], [21], instead of [17], the former having been found to be closer to measurements in proton experiments. Recently, Bohlen et al. [22] proposed an interesting study comparing nuclear fragmentation models of FLUKA and Geant4 for carbon ion therapy, and gave indications to better tune Geant4. In this study, we focused on the positron emitter production (^{11}C and ^{15}O) for dosimetry monitoring by PET imaging. As shown by Pshenichnov et al. [23], the numerical model overestimates the cross-section production of ^{11}C and ^{15}O by 15% to 20% according to measurements performed in [24]. This will be directly correlated to the PET signal with an overestimation in the same range.

3) *Scanned beam delivery system:* We considered a virtual beam delivery system inspired by the one described in [25]. Scanning is achieved with the superimposition of multiple carbon ion spots varying in lateral and longitudinal directions, and in energy. The scanning is intended to spread out the dose such that the target volume receives a uniformly high dose. Given a beam direction, the distal plane of the target volume was sampled with spots positioned every 1.5 mm. Each spot was mono-energetic, having a symmetric Gaussian profile of 5 mm FWHM, and was directed towards its end point in the distal plane. We considered energy layers every 2 mm (about 3 MeV). We defined a simple pencil beam model following [21]. We used one spot size, although in general the size should be dependent on the beam energy. More advanced descriptions of a pencil beam scanning delivery technique can be performed [26] when the focus is on a real facility. In carbon facilities, such as the Heidelberger Ionenstrahl-Therapiezentrum or the Darmstadt Helmholtz Centre for Heavy Ion Research, the radiation delivered by the synchrotron is pulsed with a spill (beam extraction) time of

less than 2 seconds and a period of about 5 seconds that is required for beam injection and acceleration.

However, we did not split the time structure in spills; we considered it instead as continuous. Likewise, we did not consider the time required to switch energy between two iso-energy slices, which is typically in the range of 1-2 s [27].

The treatment plan was composed of thousands of spots with their intensities optimised according to the method described in [25]. This method optimises the difference between the required dose and the current dose computed with tabulated Bragg peak scaled according to water equivalent path length (WEPL). The WEPL was computed for all lines going from the virtual beam source to each spot position in the distal plane and intersecting the CT voxels. Total WEPL was estimated by summing the individual WEPL along all intersected voxels weighted by the intersection length. The WEPL for a given material was computed with an approximation of the relative stopping power (to water) computed with the Bethe-Bloch formula, $wepl = \rho \frac{Z/A}{0.555}$, where Z is the atomic number, A is the mass number, and ρ is the mass density of the material. The precomputed database of depth deposited energy profiles in water, with energy from 160 MeV/u to 230 MeV/u, with a 0.05 mm depth resolution, was computed from multiple GATE simulations. The optimisation was performed field by field, with the single-field uniform-dose method [28].

We considered three fields leading to approximately 6000 individual spots. This does not correspond to real treatment plans but aims at describing a representative test case. The typical radiation dose rate is 5 GyE/min/l [29], corresponding to an intensity of 1.2×10^9 particles per seconds (pps). Regarding the proposed pencil beam description, we thus considered that 10^8 to 10^9 particles reaching the patient correspond to 1 Gy to 10 Gy in the tumour. Here we decided to focus only on the physical dose, not taking into account Relative Biological Effectiveness (RBE). Delivered dose in carbon therapy can range from 1 Gy to 10 Gy per session, for some experimental single-fraction hypofractionated treatments [30]. One irradiation takes a few minutes (according to the dose and the number of fields). We considered five different configurations, described later in Table I.

Note that the nozzle was not described in the simulation, and no contamination due to beam interactions with the material of the delivery system was included. However, prompt gamma, neutrons, and all other secondaries were simulated in the patient. If simulations must be compared with measurements, changes in the primary beam characteristics should be made. We argue, however, that this will only lead to small modifications in the dose and emitter distributions, and the principal conclusions of this study remain.

4) *Scorers*: Dose was scored with the *GATEDoseActor* described in [4], [14], which stores deposited dose and energy distribution in a 3D matrix of dosels, together with the associated statistical uncertainty. We chose a matrix of dosels of size $2^3 mm^3$. We also stored the 3D distribution of points of creation of β^+ emitters during the radiation. We limited emitters by scoring only the two main ones, ^{11}C and ^{15}O [17]; the others (^{10}C , ^{13}N , ^{14}O , $^{17,18}F$, and ^{30}P , for those with more than 10s of half-live) were considered to have negligible

influence on a reconstructed PET image, but could also be stored if needed. The energy deposited by secondary particles and specially by β^+ emitters in this case was taken into account in the dose and energy 3D matrices.

C. PET scan for dose monitoring

The conventional approach to model the PET acquisition in the case of dose monitoring for hadrontherapy applications is to convolve the β^+ emitter map with a Gaussian function determined by the point spread function of the PET system [24]. With this simplified method, scanner sensitivity is not taken into account. We think that it could be a critical point for evaluating the relation between the deposited dose and the final PET image. For this reason, we propose a full Monte Carlo simulation of the PET system. It is important to note that it is not an in-beam PET configuration, and we do not consider prompt gamma and neutron contamination during the acquisition. However, in-beam simulation of the PET system would be possible within GATE.

1) *Scanner description*: The modelled scanner for this study was the commercial ECAT EXACT HR+ [31] PET by Siemens. It is composed of four rings of bismuth germinate (BGO) blocks partially cut into an 8×8 array of crystals measuring $4.0 \times 4.1 \times 30 mm^3$ each, resulting in a 82.7 cm diameter detector cylinder and an axial field-of-view length of 15.5 cm. We defined the BGO blocks, a back compartment to simulate the back scattering induced by the light collection system, the lead endshielding, and the patient bed in the simulation. The simulation assumed an energy resolution for each crystal randomly drawn from a uniform distribution varying between 20% and 30% at 511 keV. The determination of the hit crystal was based on the crystal with the highest energy deposition, to which an additional analytical spatial blurring based on a two-dimensional Gauss kernel could be applied to model the decrease induced by the photomultiplier tubes and the Anger electronic system. A global sensitivity factor of 0.9 was defined for each block to replicate the sensitivity performance of the HR+ scanner. This PET scanner was already modelled and validated by using GATE, and all results are described in [32].

2) *PET acquisition and image reconstruction*: The energy window was set to 350-650 keV and the coincidence time window to 12 ns. The PET acquisition was started just after the radiation. The acquisition time was 10 minutes. To improve the image quantification, the simulated data were normalised and fully corrected: attenuation, scattered and random coincidences. For the reconstruction the 3D OSEM method [33] was used. To speed up the complete processing, we used the PET analytic simulator ASIM [34] with the ECAT HR+ scanner geometry description to produce the normalisation sinogram. For the attenuation correction, coefficient factors (ACFs) were also calculated with ASIM using the voxelised attenuation map description provided by the numerical patient phantom. This approach, validated in a previous work [32], allowed us to perform data corrections without modelling the acquisitions of scanner normalisation and patient transmission by using GATE.

D. Running GATE on a high performance computing machine

To demonstrate the high scalability of the platform, all the simulations were run on the TITANE supercomputer at the Computing Center for Research and Technology (CCRT). This is a cluster integrating 1596 Bull NovaScale R422 servers, with two Intel Xeon 5570 quad-core processors, each including a memory of 3 GB per core. With 3192 Intel Xeon 5570 quad-core processors, TITANE offers a processing capacity above 90 teraflops and 25 terabytes of core memory, which put it at 38th among the top 500 supercomputer sites in the world in June 2009. The TITANE cluster operates the Bull HPC software platform that includes the Linux operating system and the global and parallel Lustre file system. This platform is based on an open-source software integrated and optimised by Bulls HPC competence centre in Echirrolles, France. GATE simulations were split into similar jobs having different random seeds. Tools to allow simplified access to this kind of computing resources are under development [35]. The Mersenne-Twister random engine, with a Mersenne-prime period of $2^{19937} - 1$, is required for such a large simulation. For the imaging part, jobs are split following the PET acquisition time and including the positron emitters decay time.

E. Quantitative analysis

For this analysis, a profile was defined on a tumour with a length of 80 mm and a width of 2 mm (illustrated in Figs. 4, 5 and 6). To quantify this analysis of the PET images, we considered the distance L between the 50% distal falloff (DFO) and the peak position as illustrated in Fig. 2. We first considered three configurations corresponding to three dose values delivered to the tumour: 1, 5, and 10 Gy (S_1 , S_2 , S_3). An additional configuration, S_1^* , was performed with Gaussian smoothing to be compared with full PET system simulation (S_1). The configuration S_3^* was performed to evaluate the interest to consider the ^{15}O isotope in addition to ^{11}C . Finally, to quantify the influence of the dose on image quality, we compared the configurations S_3 , S_2 and S_1 . Table I describes the parameters of the five studied configurations.

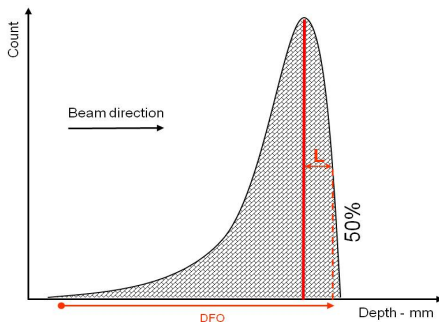


Fig. 2. Definition of the quantitative parameter: L is the distance between the 50% DFO and the peak position.

III. RESULTS AND DISCUSSION

Figure 3 illustrates the dose deposited (A) during the radiation and the β^+ emitter maps for the ^{11}C (B) and ^{15}O (C)

Simulation configuration	^{12}C number	Dose to tumor (Gy)	PET model	β^+ emitter contribution
S_1	$3 \cdot 10^8$	1	Full GATE	^{11}C
S_1^*	$3 \cdot 10^8$	1	Gaussian	^{11}C
S_2	$15 \cdot 10^8$	5	Full GATE	^{11}C
S_3	$3 \cdot 10^9$	10	Full GATE	^{11}C
S_3^*	$3 \cdot 10^9$	10	Full GATE	$^{11}\text{C} + ^{15}\text{O}$
CPU Time				
$3 \cdot 10^9$ ions of ^{12}C	20000 h.			
For full PET modelling	3600 h.			

TABLE I

Global computing time and setup description: carbon ion beam, target dose, and PET simulation approach

isotopes that were produced by ^{12}C interactions for the setup S_3 . These images represent a qualitative proof of concept of the capabilities of GATE to perform complete and realistic simulations in the field of hadrontherapy coupled with a nuclear imaging device.

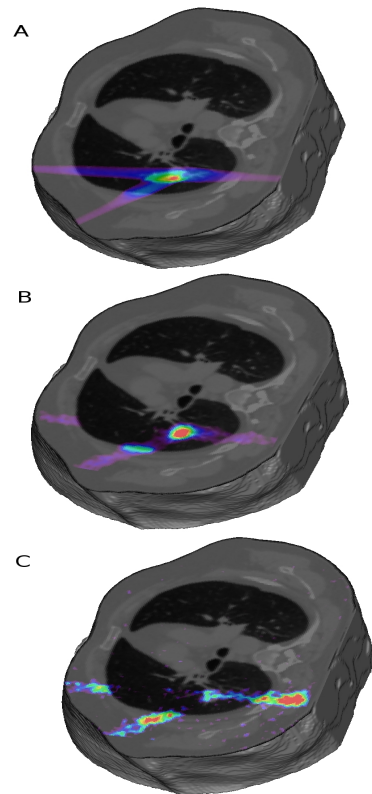


Fig. 3. Qualitative representation of our complete simulation, from the dose map to the PET images merged on the 3D CT scan: (A) illustration of the deposited dose distribution from a three-field irradiation converging to the tumour target; (B) PET image considering only the ^{11}C isotope; (C) PET image for ^{15}O .

Figure 4 compares the configurations S_1 and S_1^* to illustrate the interest to simulate the complete PET acquisition system instead of using a Gaussian smoothing. The latter method does not take into account several effects, such as material attenuation, photon scattering, limited detection solid angle, and the intrinsic detector response. All these effects influence the sensitivity of the PET camera and thus the relationship

with the deposited dose. In this case, L artificially decreases from 9 with S_1 to 7.5 mm with S_1^* , leading to a 20% difference (Table II), which demonstrates that data quantification is biased with a simplified approach to model the imaging system.

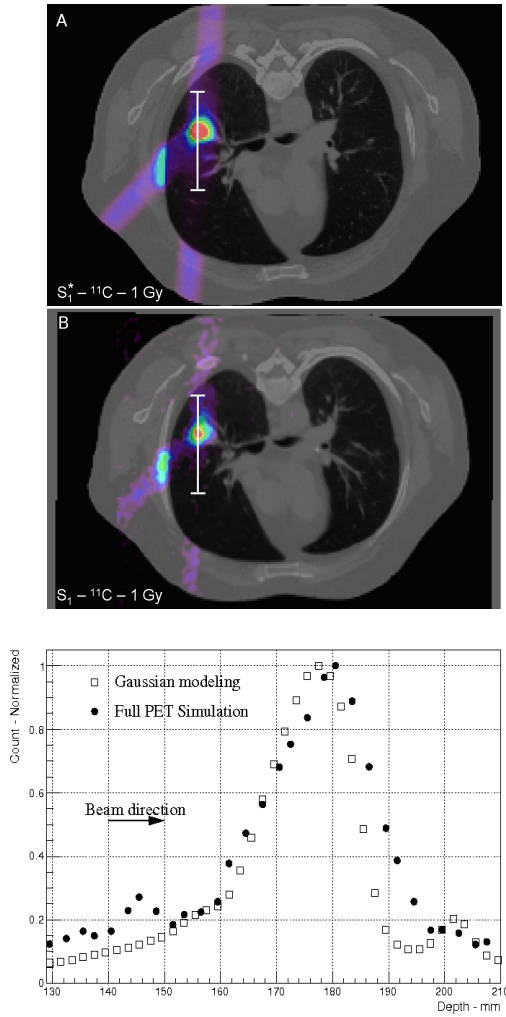


Fig. 4. Comparison between configurations S_1^* and S_1 . It illustrates the differences between the PET images obtained with Gaussian smoothing (S_1^*) and the ones obtained with a complete PET system simulated by Monte Carlo (S_1).

Configurations	L (mm)	Peak position (mm)
S_1 (full PET)	9.0	180
S_1^* (Gaussian PET)	7.5	177
$\Delta_L(S_1^*; S_1)$	20 %	

TABLE II

Quantitative differences between Gaussian-based PET modelling and full system simulation

We also studied the contribution of the ^{15}O isotope to the final PET images by comparing configurations S_3^* and S_3 . Figure 5 illustrates the differences between the two PET images. These differences were around 4.5%, as quantitatively presented in Table III. Indeed, it is known that ^{11}C production is higher than ^{15}O production by a factor of 4-5 and that the

half-life is 2 minutes for ^{15}O and 20 minutes for ^{11}C . These two effects, combined with a PET scan for 10 minutes, explain the results illustrated in Fig 5. Thus, it is not necessary at this level of knowledge to develop a dedicated method to correct the ^{11}C PET image from the ^{15}O contribution.

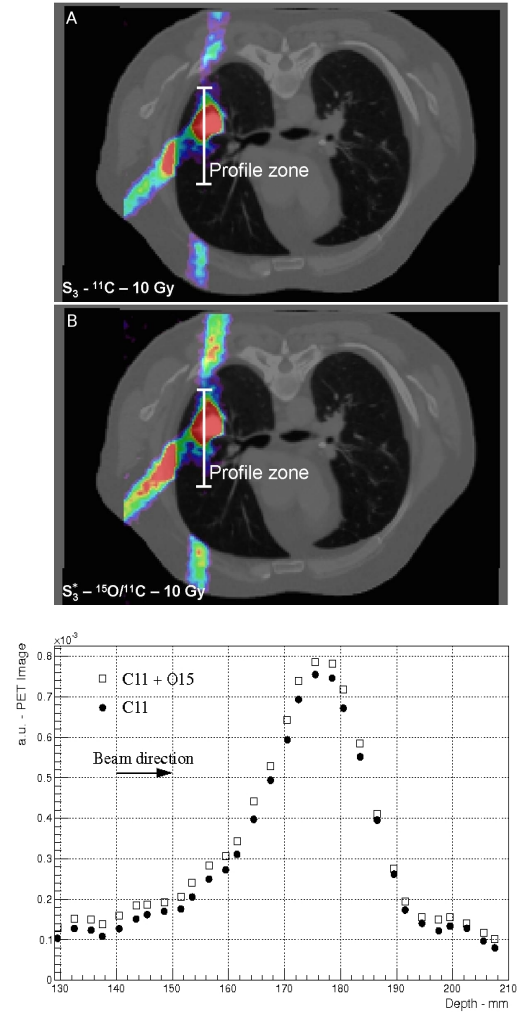


Fig. 5. Comparison between configurations S_3 and S_3^* to illustrate the influence of the ^{15}O isotope on the PET image. The top image was obtained by considering ^{11}C only, and the middle image considering both ^{11}C and ^{15}O .

Configurations	L (mm)	Max peak position (mm)
S_3 (^{11}C only)	11	176
S_3^* (^{11}C and ^{15}O)	10.5	176
$\Delta_L(S_3^*; S_3)$	4.5 %	

TABLE III

Difference between PET images obtained from ^{11}C only and from both ^{11}C and ^{15}O

The third analysis concerns the influence of the dose on PET image quality (configurations S_1 , S_2 , and S_3). Table IV and Fig. 6 show the high sensitivity to the level of delivered dose. In particular, L varies from 9 to 11 mm (22%). These results mean that care must be taken when DFO is studied from PET images.

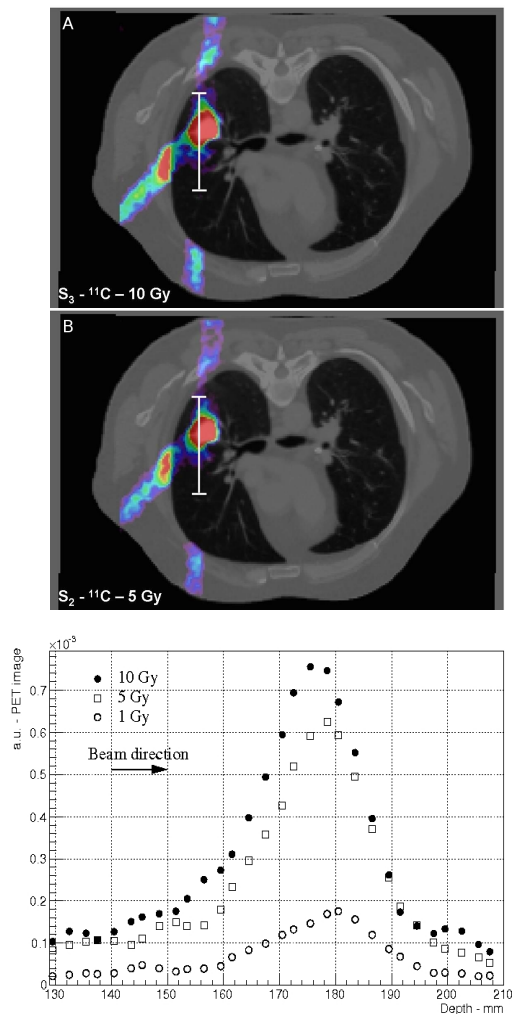


Fig. 6. Images obtained from the complete PET system simulations for 10, 5, and 1 Gy delivered to the tumour

Configurations	L (mm)	Max peak position (mm)
S_3	11	176
S_2	10	178
S_1	9	180
$\Delta_L(S_3; S_2)$		10 %
$\Delta_L(S_2; S_1)$		11 %
$\Delta_L(S_3; S_1)$		22 %

TABLE IV

Quantitative estimators to evaluate the relation between the tumour deposited dose and the ^{11}C PET image monitoring

Regarding computing time, we used 1000 CPUs for 20 hours for the radiation simulation (3.10^9 particles) and 600 processors for 6 hours for the PET simulation, for a total CPU time of 23600 hours.

As explained before, the proposed Monte Carlo simulation is realistic but does not correspond to an existing carbon delivery system. Thus, we cannot provide an evaluation against experimental data or clinical validation. However, the GATE platform has been compared against measurements and a treatment planning system in the field of protontherapy [26], [36]. It was found to be an interesting and reliable complement to

analytical codes. For example, these Monte Carlo simulations could be used as an additional dose distribution verification and as a PET image predictor that can be launched between the treatment planning and the first treatment session. However, computing time is still an issue, and powerful clusters would be needed in a clinical environment.

IV. CONCLUSION

This feasibility study illustrates the capability of GATE to perform realistic simulations in the fields of hadrontherapy and nuclear imaging for *in vivo* dose monitoring. This work shows that, thanks to the high scalability of the code, the GATE platform is well suited to produce scientific data from highly realistic simulations. It was illustrated with simulations of a complete carbon beam cancer treatment plan on a patient CT image, coupled with a full PET acquisition system used for dose monitoring. We show the importance of using a realistic model of the PET system, instead of a Gaussian function response as is generally done. Differences in the distal position of the signal falloff of 20% between full PET system simulation and the Gaussian model were found. Such simulation platform could be used to help design imaging systems for hadrontherapy, to optimise their sensitivity and quantitative performance. It could also be used to study the relationship between deposited dose and PET or prompt-gamma image.

A major challenge of hadron-PET is the detection of a low number of events. The performance of the imaging system and the image reconstruction algorithm is thus crucial. For PET data reconstruction, some approaches are focused on 4D algorithm developments [37], which include a temporal regularisation based on tracer kinetic properties. These methods, which are typically well suited in the case of low statistic acquisition, are under validation. Very realistic simulations of radiation protocols associated with the imaging system for therapeutic control will be essential to validate all these new approaches.

ACKNOWLEDGEMENTS

The authors thank the members of the OpenGATE collaboration for useful discussions.

REFERENCES

- [1] W. Enghardt, J. Debus, T. Haberer, B. G. Hasch, R. Hinz, O. Jäkel, M. Krämer, K. Lauckner, and J. Pawelke, "The application of PET to quality assurance of heavy-ion tumor therapy." *Strahlentherapie und Onkologie : Organ der Deutschen Röntgengesellschaft ... [et al]*, vol. 175 Suppl, pp. 33–6, Jun. 1999.
- [2] D. Rogers, "Fifty years of Monte Carlo simulations for medical physics." *Phys Med Biol*, vol. 51, no. 13, pp. R287–301, 2006. [Online]. Available: <http://www.ncbi.nlm.nih.gov/pubmed/16790908>
- [3] S. Jan, G. Santin, D. Strul, S. Staelens, K. Assié, D. Autret, S. Avner, R. Barbier, M. Bardiès, P. M. Bloomfield, D. Brasse, V. Breton, P. Bruyndonckx, I. Buvat, A. F. Chatzioannou, Y. Choi, Y. H. Chung, C. Comtat, D. Donnarieix, L. Ferrer, S. J. Glick, C. J. Groiselle, D. Guez, P.-F. Honore, S. Kerhoas-Cavata, A. S. Kirov, V. Kohli, M. Koole, M. Krieguer, D. J. van der Laan, F. Lamare, G. Langeron, C. Lartzien, D. Lazaro, M. C. Maas, L. Maigne, F. Mayet, F. Melot, C. Merheb, E. Pennacchio, J. Perez, U. Pietrzyk, F. R. Rannou, M. Rey, D. R. Schaart, C. R. Schmidlein, L. Simon, T. Y. Song, J.-M. Vieira, D. Visvikis, R. Van de Walle, E. Wieërs, and C. Morel, "GATE: a simulation toolkit for PET and SPECT," *Physics in Medicine and Biology*, vol. 49, pp. 4543–4561, Oct. 2004.

- [4] S. Jan, D. Benoit, E. Becheva, T. Carlier, F. Cassol, P. Descourt, T. Frisson, L. Grevillot, L. Guigues, T. Maigne, C. Morel, Y. Perrot, N. Rehfeld, D. Sarrut, D. R. Schaart, S. Stute, U. Pietrzyk, D. Visvikis, N. Zahra, and I. Buvat, "GATE V6: a major enhancement of the GATE simulation platform enabling modelling of CT and radiotherapy." *Physics in medicine and biology*, vol. 56, no. 4, pp. 881–901, Jan. 2011.
- [5] J. Allison, K. Amako, J. Apostolakis, H. Araujo, P. Arce Dubois, M. Asai, G. Barrand, R. Capra, S. Chauvie, R. Chytraccek, G. Cirrone, G. Cooperman, G. Cosmo, G. Cuttone, G. Daquino, M. Donszelmann, M. Dressel, G. Folger, F. Foppiano, J. Generowicz, V. Grichine, S. Guatelli, P. Gumplinger, A. Heikkinen, I. Hrivnacova, A. Howard, S. Incerti, V. Ivanchenko, T. Johnson, F. Jones, T. Koi, R. Kokoulin, M. Kossov, H. Kurashige, V. Lara, S. Larsson, F. Lei, O. Link, F. Longo, M. Maire, A. Mantero, B. Mascialino, I. McLaren, P. Mendez Lorenzo, K. Minamimoto, K. Murakami, P. Nieminen, L. Pandola, S. Parlati, L. Peralta, J. Perl, A. Pfeiffer, M. Pia, A. Ribon, P. Rodrigues, G. Russo, S. Sadilov, G. Santin, T. Sasaki, D. Smith, N. Starkov, S. Tanaka, E. Tchernaev, B. Tome, A. Trindade, P. Truscott, L. Urban, M. Verderi, A. Walkden, J. Wellisch, D. Williams, D. Wright, and H. Yoshida, "Geant4 developments and applications." *IEEE Transactions on Nuclear Science*, vol. 53, no. 1, pp. 270–278, Feb. 2006.
- [6] S. Agostinelli, "Geant4 - a simulation toolkit." *Nuclear Instruments and Methods in Physics Research Section A: Accelerators, Spectrometers, Detectors and Associated Equipment*, vol. 506, no. 3, pp. 250–303, Jul. 2003.
- [7] M. Moteabbed, S. Espana, and H. Paganetti, "Monte Carlo patient study on the comparison of prompt gamma and PET imaging for range verification in proton therapy." *Physics in medicine and biology*, vol. 56, no. 4, pp. 1063–82, Feb. 2011.
- [8] K. Parodi, T. Bortfeld, and T. Haberer, "Comparison between in-beam and offline positron emission tomography imaging of proton and carbon ion therapeutic irradiation at synchrotron- and cyclotron-based facilities." *International journal of radiation oncology, biology, physics*, vol. 71, no. 3, pp. 945–56, Jul. 2008.
- [9] I. Buvat and D. Lazaro, "Monte Carlo simulations in emission tomography and GATE: An overview." *Nuclear Instruments and Methods in Physics Research Section A: Accelerators, Spectrometers, Detectors and Associated Equipment*, vol. 569, no. 2, pp. 323–329, Dec. 2006.
- [10] E. Seravalli, C. Robert, J. Bauer, F. Stichelbaut, C. Kurz, J. Smeets, C. Van Ngoc Ty, D. R. Schaart, I. Buvat, K. Parodi, and F. Verhaegen, "Monte Carlo calculations of positron emitter yields in proton radiotherapy." *Physics in medicine and biology*, vol. 57, no. 6, pp. 1659–1673, Mar. 2012.
- [11] L. Grevillot, D. Bertrand, F. Dessy, N. Freud, and D. Sarrut, "A Monte Carlo pencil beam scanning model for proton treatment plan simulation using GATE/GEANT4." *Physics in Medicine and Biology*, vol. 56, no. 16, pp. 5203–5219, Aug. 2011.
- [12] E. Testa, M. Bajard, M. Chevallier, D. Dauvergne, F. Le Foulher, N. Freud, J. Létang, J. Poizat, C. Ray, and M. Testa, "Monitoring the Bragg peak location of 73 MeV/u carbon ions by means of prompt-gamma-ray measurements." *Applied physics letters*, vol. 93, p. 093506, 2008.
- [13] J. Vandemeulebroucke, O. Bernard, S. Rit, J. Kybic, P. Clarysse, and D. Sarrut, "Automated segmentation of a motion mask to preserve sliding motion in deformable registration of thoracic CT." *Medical physics*, vol. 39, no. 2, p. 1006, Feb. 2012.
- [14] D. Sarrut and L. Guigues, "Region-oriented CT image representation for reducing computing time of Monte Carlo simulations." *Medical Physics*, vol. 35, no. 4, p. 1452, 2008.
- [15] W. Schneider, T. Bortfeld, and W. Schlegel, "Correlation between CT numbers and tissue parameters needed for Monte Carlo simulations of clinical dose distributions." *Physics in medicine and biology*, vol. 45, no. 2, pp. 459–478, 2000.
- [16] Geant4 Electromagnetic Standard Working Group, "http://geant4.cern.ch/support/source/bck/geant4/collaboration/working_groups/electromagnetic/index.shtml," 2010.
- [17] I. Pshenichnov, A. Larionov, I. Mishustin, and W. Greiner, "PET monitoring of cancer therapy with 3He and 12C beams: a study with the GEANT4 toolkit." *Physics in medicine and biology*, vol. 52, no. 24, pp. 7295–312, Dec. 2007.
- [18] C. Zacharitou-Jarlskog and H. Paganetti, "Physics Settings for Using the Geant4 Toolkit in Proton Therapy." *IEEE Transactions on Nuclear Science*, vol. 55, no. 3, pp. 1018–1025, Jun. 2008.
- [19] J. C. Polf, S. Peterson, M. McCleskey, B. T. Roeder, A. Spiridon, S. Beddar, and L. Trache, "Measurement and calculation of characteristic prompt gamma ray spectra emitted during proton irradiation." *Physics in medicine and biology*, vol. 54, no. 22, pp. N519–27, Nov. 2009.
- [20] S. W. Peterson, J. Polf, M. Bues, G. Ciangaru, L. Archambault, S. Beddar, and A. Smith, "Experimental validation of a Monte Carlo proton therapy nozzle model incorporating magnetically steered protons." *Physics in medicine and biology*, vol. 54, no. 10, pp. 3217–29, May 2009.
- [21] L. Grevillot, T. Frisson, N. Zahra, D. Bertrand, F. Stichelbaut, N. Freud, and D. Sarrut, "Optimization of GEANT4 settings for Proton Pencil Beam Scanning simulations using GATE." *Nuclear Instruments and Methods in Physics Research Section B: Beam Interactions with Materials and Atoms*, vol. 268, pp. 3295–3305, Aug. 2010.
- [22] T. Böhlen, F. Cerutti, M. Dosanjh, A. Ferrari, I. Gudowska, A. Mairani, and J. Quesada, "Benchmarking nuclear models of FLUKA and GEANT4 for carbon ion therapy." *Physics in medicine and biology*, vol. 55, no. 19, pp. 5833–47, Oct. 2010.
- [23] I. Pshenichnov, I. Mishustin, and W. Greiner, "Distributions of positron-emitting nuclei in proton and carbon-ion therapy studied with GEANT4." *Physics in medicine and biology*, vol. 51, no. 23, pp. 6099–112, 2006.
- [24] K. Parodi, A. Ferrari, F. Sommerer, and H. Paganetti, "A MC tool for CT-based calculations of dose delivery and activation in proton therapy." in *First European Workshop on Monte-Carlo Treatment Planning*, vol. 74. IOP Publishing, 2007, p. 021013.
- [25] M. Krämer, O. Jäkel, T. Haberer, G. Kraft, D. Scharadt, and U. Weber, "Treatment planning for heavy-ion radiotherapy: physical beam model and dose optimization." *Physics in Medicine and Biology*, vol. 45, p. 3299, 2000.
- [26] L. Grevillot, T. Frisson, D. Maneval, N. Zahra, J. J.-N. J. Badel, and D. Sarrut, "Simulation of a 6 MV Elekta Precise Linac photon beam using GATE/GEANT4." *Physics in Medicine and Biology*, vol. 56, no. 4, p. 903, Jan. 2011.
- [27] E. Rietzel and C. Bert, "Respiratory motion management in pArticle therapy." *Medical Physics*, vol. 37, no. 2, p. 449, 2010.
- [28] A. Lomax, "Intensity modulation methods for proton radiotherapy." *Physics Medicine Biology*, vol. 44, no. 1, pp. 185–205, Jan. 1999.
- [29] K. Noda, T. Furukawa, T. Fujisawa, Y. Iwata, T. Kanai, M. Kanazawa, A. Kitagawa, M. Komori, S. Minohara, T. Murakami, M. Muramatsu, S. Sato, Y. Takei, M. Tashiro, M. Torikoshi, S. Yamada, and K. Yusa, "New Accelerator Facility for Carbon-Ion Cancer-Therapy." *Journal of Radiation Research*, vol. 48, no. Suppl.A, pp. A43–A54, 2007.
- [30] H. Tsujii, T. Kamada, M. Baba, H. Tsuji, H. Kato, S. Kato, S. Yamada, S. Yasuda, T. Yanagi, H. Kato, R. Hara, N. Yamamoto, and J. Mizoe, "Clinical advantages of carbon-ion radiotherapy." *New Journal of Physics*, vol. 10, no. 7, p. 075009, Jul. 2008.
- [31] G. Brix, J. Zaers, L. Adam, M. Bellemann, H. Ostertag, H. Trojan, U. Haberkorn, J. Doll, F. Oberdorfer, and W. Lorenz, "Performance Evaluation of a Whole-Body PET Scanner Using the NEMA Protocol." *J.Nucl. Med.*, vol. 38, pp. 1614– 1623, 1997.
- [32] S. Jan, C. Comtat, D. Strul, G. Santin, and R. Trébosse, "Monte Carlo Simulation for the ECAT EXACT HR+ system using GATE." *IEEE Transactions Nuclear Science*, vol. 52, pp. 627– 633, 2005.
- [33] H. Hudson and R. S. Larkin, "Accelerated image reconstruction using ordered subsets of projection data." *IEEE Transactions Medical Imaging*, vol. 13, pp. 601– 610, 1994.
- [34] C. Comtat, P. Kinahan, M. Defrise, C. Michel, C. Lartizien, and D. Townsend, "Simulating whole-body PET scanning with rapid analytical methods." *Proceedings IEEE Medical Imaging Conference*, vol. 3, pp. 1260– 1264, 1999.
- [35] S. Camarasu-Pop, T. Glatard, J. T. Mościcki, H. Benoit-Cattin, and D. Sarrut, "Dynamic Partitioning of GATE Monte-Carlo Simulations on EGEE." *Journal of Grid Computing*, vol. 8, no. 2, pp. 241–259, Mar. 2010.
- [36] L. Grevillot, D. Bertrand, F. Dessy, N. Freud, and D. Sarrut, "GATE as a GEANT4-based Monte Carlo platform for the evaluation of proton pencil beam scanning treatment plans." *Physics in Medicine and Biology*, vol. 57, no. 13, pp. 4223–4244, Jul. 2012.
- [37] M. Fall, E. Barat, C. Comtat, T. Dautremer, T. Montagu, and A. Mohammad-Djafari, "Continuous space-time reconstruction in 4D PET." *Proceedings IEEE Medical Imaging Conference*, 2011.